

Cross-scale analysis of the energy recovery process in pressure exchanger and pipeline system

Zheng Cao, Jianqiang Deng*, Fanghua Ye

School of Chemical Engineering and Technology, Xi'an Jiaotong University, Xi'an 710049, Shaanxi, China, Tel. +86 29 82663413; Fax: +86 29 82663413; emails: dengjq@xjtu.edu.cn (J. Deng), zhengcao@xjtu.edu.cn (Z. Cao), jkzx4416176@stu.xjtu.edu.cn (F. Ye)

Received 27 July 2018; Accepted 21 July 2019

ABSTRACT

The pressure exchanger is a key component in the seawater reverse osmosis system. This work focused on the one-dimensional and three-dimensional co-simulation between device and pipeline scale. The coupling calculation was carried out by combining the method of characteristic with computational fluid dynamics through the self-programming platform, with satisfying accuracy and computational efficiency. With the extracted modeling data, the pressure surge under transient operating conditions was evaluated. Several methods suppressed the pressure fluctuation of the pipeline under transient conditions were presented. The effects of flow arrangement and valve closure schemes on hydraulic performance were discussed based on a subsystem simulation case. The calculation results showed that the correction factor and initial pressure value are the main factors that largely affect the convergence process in the co-simulation. The calculated pressure loss in the high-pressure area and low-pressure area of the rotary pressure exchanger are about 0.13 and 0.073 MPa, respectively. As for the hydraulic transient control, valve closure time was the most obvious effect on pressure fluctuation. When operated at an optimum fast closure rate of 60%, the fast-slow valve closure scheme can be applied for reducing pressure peak to the minimum. In addition, the U flow arrangement was recommended in process design for higher energy transfer efficiency as well as lower pressure surge.

Keywords: Rotary pressure exchanger; Energy recovery; Co-simulation; Pressure suppression; SWRO

1. Introduction

Energy-saving is a key topic in the energy-intensive desalination process. As one of the most efficient energy-saving processes, seawater reverse osmosis (SWRO) is widely used in seawater desalination plants [1,2]. In such a process, the rotary pressure exchanger (RPE) acts as an isobaric energy recovery device, which helps decrease energy consumption by up to 60% accompanied by its high device efficiency [3].

Fig. 1 shows a typical SWRO process with the application of RPE. The SWRO system consists of a seawater pump, a high-pressure pump, a booster pump, reverse osmosis (RO) membrane modules, and an RPE device. The RPE device recovers the pressure of high-pressure fluid from the RO

membrane to pressurize parts of seawater in the recycle loop, then the depressurized fluid discharges from the system. A booster pump supplies for the pressurized seawater due to the pressure loss in the RO membrane, RPE device, and pipelines, then the fully pressurized seawater flows to the RO membrane together with the seawater pumped by the high-pressure pump.

Since the pressure exchanger plays an important role in the energy recovery process, much research has been focused on the advanced design for a better hydraulic performance termed as energy recovery efficiency and mixing rate. Xu et al. [4] investigated the effects of operating conditions on mixing performance of a four-port RPE by using computational fluid dynamics (CFD) method, and they observed a

* Corresponding author.

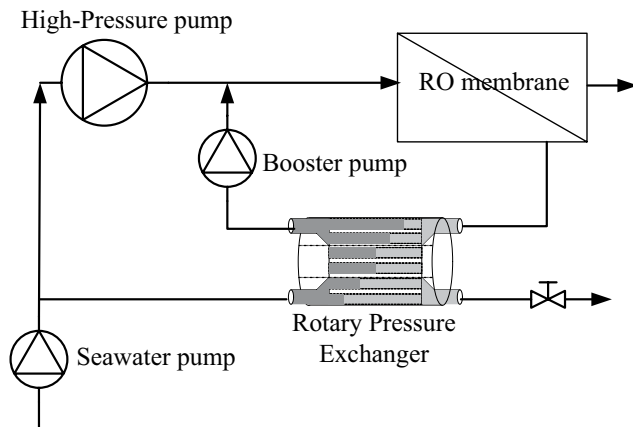


Fig. 1. Schematic view of the typical SWRO process with RPE.

polynomial relation between mixing rate and dimensionless inflow length. Liu et al. [5] studied the flow structure in rotor ducts, and the numerical results showed that the flow turbulence and mass transfer in the mixing zone were caused by swirling flow. Jiao et al. [6] obtained an approximately linear relationship between pressure loss rate and working conditions from the regression analysis of the experiment, and following steady-state numerical simulation showed an acceptable data error with the empirical formula. Al-Hawaj [7] introduced a sliding-vane work exchanger, and theoretical analysis on the device performance was carried out to prove its feasible application in the SWRO system. Ye et al. [8] proposed a cylinder profile model, and the parametric analysis suggested that the sliding vane type device is promising in the energy recovery process. Cao et al. [9] introduced a disc-type pressure exchanger, which combined both characteristics of positive displacement and centrifugal type pressure exchangers to achieve a pressure boost effect. Liu et al. [10] proposed a rotary valve pressure exchanger, and an optimization study on the seal structure indicated the device efficiency could reach to 96.33% with a relaxed requirement for clearance. Wang et al. [11] introduced pre-pressurization/depressurization grooves on RPE end cover, the numerical results showed a significant decrease in flow and pressure fluctuations caused by RPE rotation.

Although numerical simulation has been widely used in flow field analysis of standalone RPE devices, a full size of three-dimensional (3D) CFD model is time-consuming and inefficient to describe the system characteristics under a larger device-pipeline scale. On the other hand, the commonly used one-dimensional (1D) or zero-dimensional equivalent model is not able to predict flow information with satisfied computational accuracy. Hence, it is necessary to employ a cross-scale simulation, where the fluid flow inside the device and pipeline system are characterized by a 3D CFD model and 1D simplified model, respectively. Such joint simulation can obtain a good balance in computational efficiency and accuracy, as well as flow field information of the specified device. As an example, the German BMW successfully applied a 1D and 3D co-simulation to the design of the cooling system, and the coupling calculation resulted in a 14% change in the flow split and 4% reduction in overall flow, which is more accurate compared to the conventional CFD result [12].

This work aims to introduce the cross-scale co-simulation method applied in the energy recovery process and to analyze the control approach of the transient flow phenomenon in the pipeline system. In this case, a 1D-3D co-simulation was realized in the pipeline system equipped with RPE. By using the self-developed interface code, the joint simulation based on the method of characteristic (MOC-CFD) model was carried out at a steady state. The obtained results satisfied with calculation efficiency and engineering accuracy, and the numerical factors affecting the calculation results were also investigated. Moreover, a 1D transient analysis was conducted with the extracted modeling data, the pressure surge under transient operating condition was evaluated, and several methods for suppressing the pressure fluctuation of the pipeline under transient conditions were presented. Furthermore, a subsystem case was introduced to evaluate the RPE arrangements effects and valve operation schemes on hydraulic performance and transient control.

2. Simulation of cross-scale pressure exchange process

2.1. Cross-scale model

In difference with the CFD method solving conservation equations of fluid flow, the MOC method is a concise discretization method used for solving transient flow equations along with the characteristic line in the time-space grid. As an exploratory study in the cross-scale co-simulation method in the energy recovery process, this work couples the 1D MOC model of the pipeline system with the 3D CFD model of the RPE device. For the 1D pipeline system, the pipe flow model was solved by using the MOC method via Flowmaster V7 software. It is an advanced computer-aided engineering/CFD tool used in modeling hydraulic problems in complex systems. With a rich components database supported by experimental data, this efficient tool has been widely used in hydraulic system design. For the 3D RPE device, the mesh was generated in GAMBIT with a grid number of 582680. The main parameters are set as follows: rotor length is 150 mm, duct diameter is 15 mm, and the end cover height is 10 mm. The CFD model was solved in a control volume discretization method by ANSYS FLUENT 14.5. The moving reference frame method is applied to the RPE rotor domain at a constant rotational speed of 500 r/min. The pressure outlet and mass flow inlet conditions are assigned to outlets and inlets on the RPE end cover correspondingly.

The diagram of the 1D pipeline and 3D RPE coupling system is shown in Fig. 2. Two pipelines with a length of 110 m are connected to the RPE high-pressure area and low-pressure area, and the pipe upstream and downstream are connected to constant pressure sources. Two ball valves are installed downstream of two pipelines, and the valve action can be regulated by the controller. In the RPE coupling position, the pressure source components P are connected to RPE flow inlets, and the flow source components F are connected to RPE pressure outlets. It should be noted that the biofouling and mixing effects are neglected in the simulation model. Considering the biofouling is a relatively long process that mainly affects the RO membrane in terms of permeability and salt rejection [13], and no obvious correlation is found

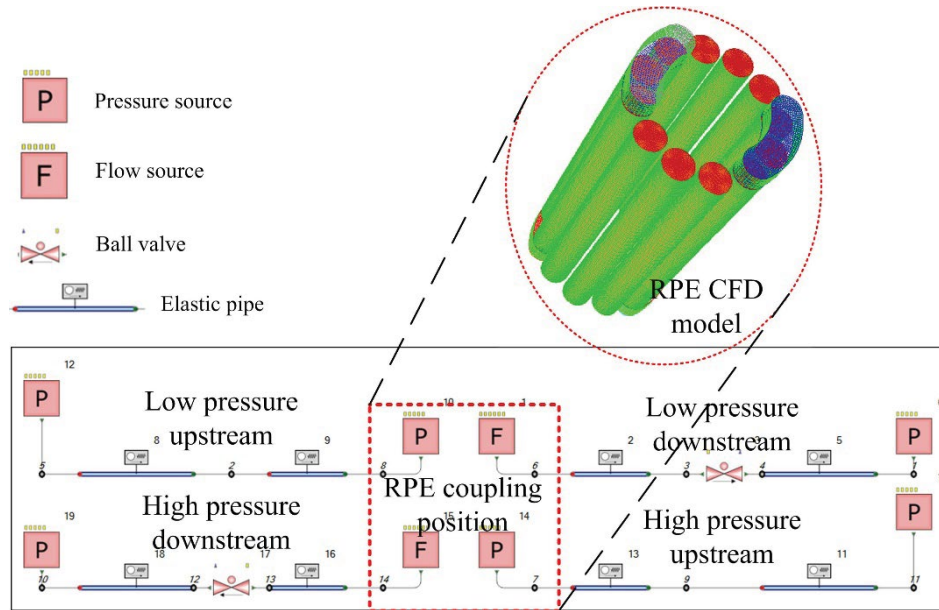


Fig. 2. Diagram of 1D pipeline and 3D RPE coupling system.

between mixing and energy recovery efficiency, the fluid is therefore assumed as water with no salt when flow behavior is mainly discussed.

2.2. Coupling method

For the cross-scale co-simulation, the variables including mass, pressure, and velocity in the flow field of RPE are calculated via the 3D CFD model. While the pipe flow in the connecting pipelines is calculated by using a 1D MOC model. The two computational domains exchange the simulation data through the coupling surface, reflecting the interactive effect between the RPE and the connecting pipeline system.

Compared with the traditional numerical simulation method, the co-simulation can reduce the number of parameter assumptions given to the border condition, and can ensure the simulation contained with flow field scale information at a high computational efficiency for long pipelines. To realize the interaction of simulation data, the Visual Basic (VB) platform is developed as a front running program to call the 1D hydraulic system code and 3D CFD code.

The data exchange through the interface between models in different dimension is the core process of coupling simulation. For data on the 1D node interface, the mass flow, m^{1D} , and pressure, p^{1D} , can be expressed as

$$m^{1D} = \sum_{j=0}^{j=n} m_j^{3D} \tag{1}$$

$$p^{1D} = \sum_{j=0}^{j=n} p_j^{3D} \times \frac{a_j^{3D}}{A} \tag{2}$$

where j is an element of 3D surface, n is the total number of surface elements, A is the area of 3D surface, a is the element area.

Conversely, when boundary data of the 1D node is known, the mass flow, m^{3D} , and pressure, p^{3D} , of 3D CFD interface can be calculated

$$m_j^{3D} = m^{1D} \times \frac{a_j^{3D}}{A} \tag{3}$$

$$p_j^{3D} = p^{1D} \tag{4}$$

In this work, the sequential bidirectional coupling scheme is employed for the MOC–CFD model. In this coupling scheme, each model in different dimensions are solved separately at first, one of the code results is set as given condition for trial calculation, and then receiving the feedback result from the other code calculation to complete one interaction process. Fig. 3 illustrates the data transfer direction in the coupling model. As shown, the pressure source and flow source elements are chosen as the data interface for the 1D Flowmaster calculation. Among them, the pressure source element “P” transfers mass flow data to the CFD model while receiving the total pressure simultaneously. At the same time, the flow source element “F” transfers to the total pressure while receiving the mass flow data from the CFD model. In this way, the boundary conditions of 1D and 3D models are updated with the transferring interface data until the coupling results meet with the required computational accuracy.

Fig. 4 shows the calculation process of the coupling model. As can be seen, the coupling calculation is completed by calling the Fluent subroutine and the Flowmaster subroutine on the VB platform. The initial mass flow rate is firstly assumed as an inlet boundary condition and is assigned to the Fluent simulation by the control of the scheme format file. Then the calculated inlet pressure is transferred to the

Flowmaster simulation controlled by the Flowmaster automation program. After the mass flow rate is obtained, a comparison with the initial assumed value will be made, and the calculation results will be outputted when the convergence criterion is satisfied.

If the convergence conditions are not satisfied, the updating of boundary conditions is required. In this work, the following equation is adopted as the boundary updating method:

$$M_{3D}^{i+1} = (1 - \gamma)M_{3D}^i + \gamma M_{1D}^i \quad (1 < \gamma < 0) \tag{5}$$

In the equation above, M is the mass flow rate, γ is the correction factor, which is used to regulate the initial value assigned to the next iteration. The superscript i and $i + 1$ represent the current iteration step and the next iteration step. The subscript 1D and 3D represent for 1D MOC model and the 3D CFD model.

In the coupling calculation, the correction factor has a critical impact on the accuracy and efficiency of the calculation

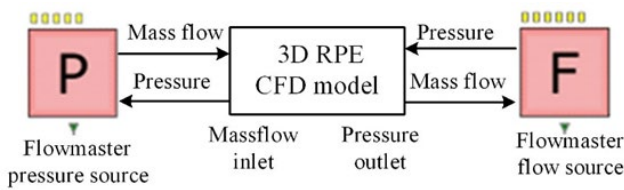


Fig. 3. Interaction framework of the coupling model.

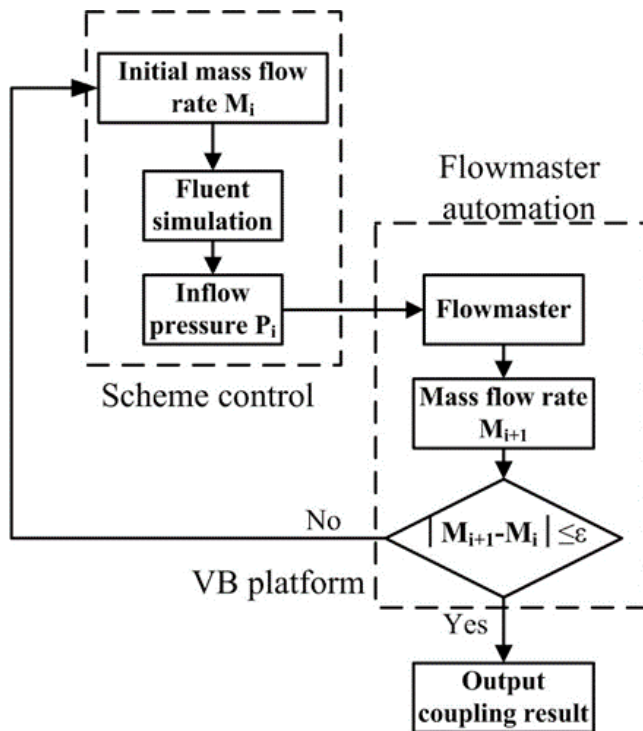


Fig. 4. Calculation process of the coupling model.

process. The co-simulation starts with setting an initial flow rate at the entrance of the CFD model, then the converged CFD pressure value is returned to the 1D MOC model to calculate the pipe flow data. Considering the flow as the conserved quantity in both CFD and MOC models, the mass flow rate is set as the evaluating parameter for calculation convergence, and the residual is set as 0.1 kg/s in flow difference for high-pressure and low-pressure areas.

3. Results and discussion

3.1. Model validation

To confirm the reliability of the co-simulation result, a numerical validation has been made by using PX-220 geometrical configuration [14]. The main size of the simulation model follows approximately the design feature as some parameters are not disclosed. In consistent with the steady working conditions of a plant test, the energy recovery efficiency is calculated and compared to the practical value. The energy recovery efficiency, η is defined as a ratio of total energy output to total energy input, as indicated in Eq. (6).

$$\eta = \frac{\sum (\text{Pressure} \times \text{Flow})_{\text{out}}}{\sum (\text{Pressure} \times \text{Flow})_{\text{in}}} \tag{6}$$

The PX device operates at a flow rate of 41 m³/h with a rotation of 825 rpm, the pressures of the high-pressure outlet and low-pressure outlet are set to 6 and 0.2 MPa, respectively. As can be seen from Fig. 5, the stand-alone CFD simulation of PX-220 operating in steady condition has an energy transfer efficiency of 99.82%, while efficiency of 96.78% is obtained using the 1D-3D co-simulation method, which is closer to the practical value of 95.1%. It is observed that the co-simulation result is overall reasonable and agrees with the published test data, the small inconsistency of a higher efficiency value in simulation result may be caused by no leakage assumption and the simplification of the geometric model. It is mentioned that although the validation model is of different sizes with the RPE models used in our work, the working principle

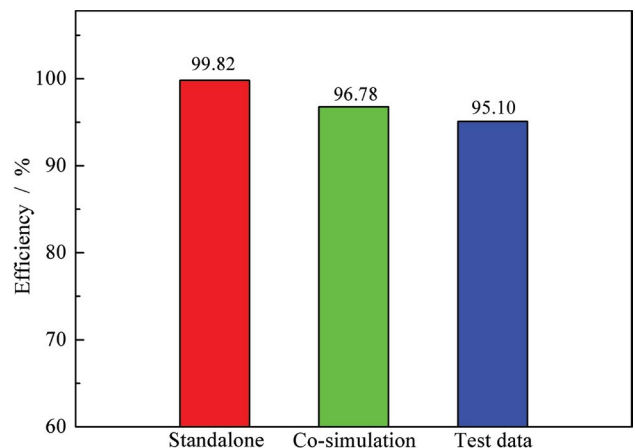


Fig. 5. Comparison between simulation results and test data.

and pressure exchange process are identical. Therefore, the validation results can be used to confirm the accuracy of the numerical model co-simulation method in this study.

3.2. Coupling calculation results

The analysis of the coupling system under steady-state conditions is the basis of other transient analysis and is an important method to characterize the stable flow of the coupling system. As a special case of unsteady problems, the calculation model under steady conditions also follows the derivation and calculation process of flow equations. As a discussion of the co-simulation method between the RPE and pipeline system, the coupling calculation under constant conditions is carried out. The key parameter settings used in co-simulation are presented in Table 1.

Fig. 6 shows the influence of correction factors on the calculation convergence. It can be seen that, during the coupling calculation, the high-pressure area represented by the dotted line and the low-pressure area represented by the real line have an approximate convergence trend. At the same time, the value of the correction factor can cause a great influence on the calculation process. When the correction factor is set to 0.2 and 0.3, the calculation is hard to converge. It is found the convergence is the best at the value of 0.1, with a less

required number of iteration steps compared to the value of 0.05. Therefore, 0.1 was selected as the correction factor for the calculation.

In addition to the calculation factor, a reasonable initial value is important for co-simulation as it is the key factor affecting the calculation convergence. Fig. 7 shows the effect of initial inlet flow values on the calculation results. The initial flow values for the case 1–3 are set as 6.5, 12.5 and 18.5 kg/s, respectively. As can be seen, even though the residual flow difference is set to 0.1 kg/s, when the calculated values of the high-pressure zone and low-pressure zone meet the convergence conditions, the flow difference is only between 0.004–0.021 kg/s, indicating an acceptable accuracy. For simulation case 1 with an initial flow value of 6.5 kg/s, it takes the shortest time to converge by 0.21 h, while for case 2 and case 3, the convergence of coupling calculation takes about 0.35 and 0.34 h, respectively. It is also seen that the pressure drop results are almost consistent when the calculation is converged. It means that the initial flow value has no obvious effect on the calculation results. The pressure drop for the RPE in the high-pressure area is about 0.136 MPa and is about 0.073 MPa for the low-pressure area.

Fig. 8 shows the effect of initial outlet pressure values on the calculation results. For cases, 4–6, the outlet pressure at high-pressure and low-pressure areas is set as 6 MPa–1 MPa, 5.95 MPa–1 MPa, 6.02 MPa–1.05 MPa, with a flow rate of 6.5 kg/s. It is seen that the flowrate difference is only between 0.004 kg/s–0.021 kg/s, which is also very small as the calculation is converged. Case 5 takes the shortest time to converge by 0.13 h, while case 6 takes a long time more than 0.44 h. In addition, when the high and low outlet pressure is set as 6.1 MPa–1.1 MPa, respectively, the calculation has diverged. This proves that it is necessary to set a reasonable initial pressure value in the coupling calculation, which will also affect the convergence of the calculation. In the converged calculation cases, there is no significant difference between the results. The pressure drop in the high-pressure area of RPE

Table 1
Parameter settings for the co-simulation model

Parameter setting	Values
Correction factor	0.1
Mass flow rate at low-pressure inlet/m s ⁻¹	12.5
Mass flow rate at high-pressure inlet/m s ⁻¹	12.5
Pressure at low-pressure outlet/MPa	1
Pressure at high-pressure outlet/MPa	6

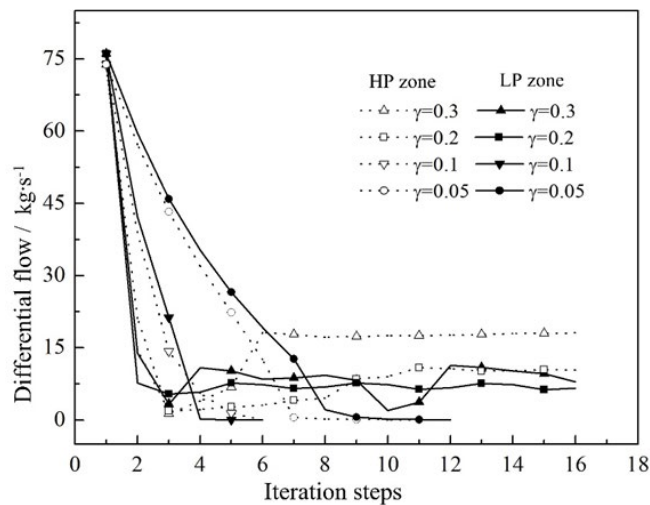


Fig. 6. Influence of correction factors on the calculation convergence.

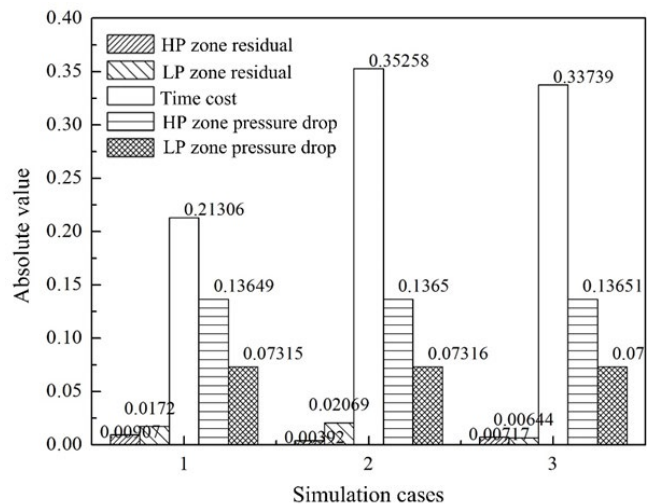


Fig. 7. Influence of initial inlet flow values on the calculation.

is about 0.13 MPa, while in the low-pressure area is about 0.073 MPa.

3.3. Pressure fluctuation under transient operation

For a pipeline system containing the RPE device, the coupling calculation can provide pressure loss data for simplifying the RPE model into a resistance component. Such an extracted modeling method can be used efficiently for the calculation of large scale pipe networks under transient conditions. With the calculation of pressure fluctuation at key nodes in the pipe system, the effect of transient phenomena such as water hammer can be evaluated during the system design process.

This work mainly focuses on the research method, therefore a relatively simple pipeline model is developed, where the energy recovery device is replaced by an equivalent

resistance component. The pressure drop data is extracted by the test data [15], the relationship between pressure drop and flow is as shown in Fig. 9. It can be seen that under the same flow rate, the pressure drop in the high-pressure area is always higher than that in the low-pressure area.

To study the effect of transient operation effects on RPE pipelines, a simple pipeline connection is set in Fig. 10. As is shown, the high-pressure pipeline followed by a centrifugal pump is connected to a water tank with a water head of 77 m. The low-pressure source for the pipeline is provided by a water tank with a water head of 9 m. Two ball valves are located downstream of the high-pressure pipeline and the low-pressure pipeline respectively. To investigate the effect of valve action on pipeline pressure fluctuation, the fast closure is set as valve opening from 1.0 at 0.39 s to 0.1 in 0.01 s, and the slow closure is set as valve opening from 1.0 at 0.39 s to 0.1 in 0.3 s.

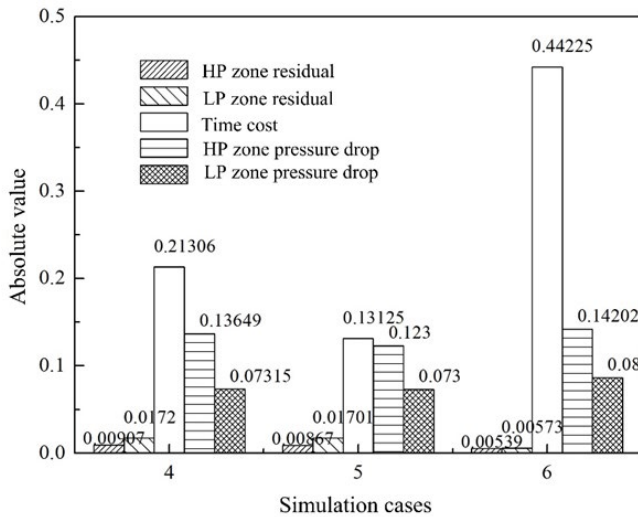


Fig. 8. Influence of initial outlet pressure values on the calculation.

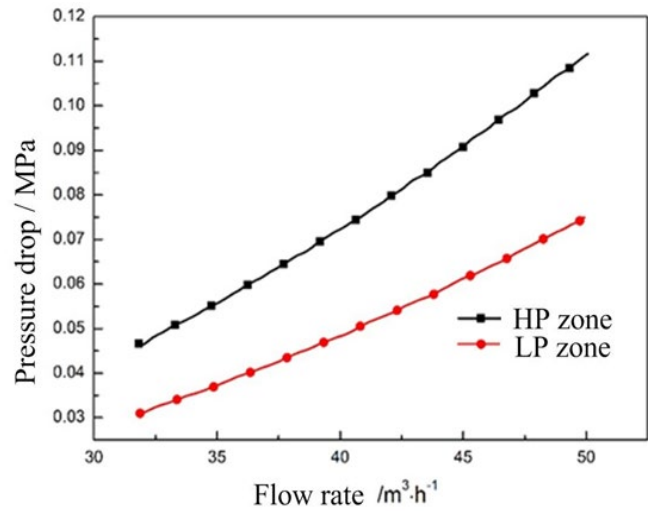


Fig. 9. Relationship between pressure drop and flow rate.

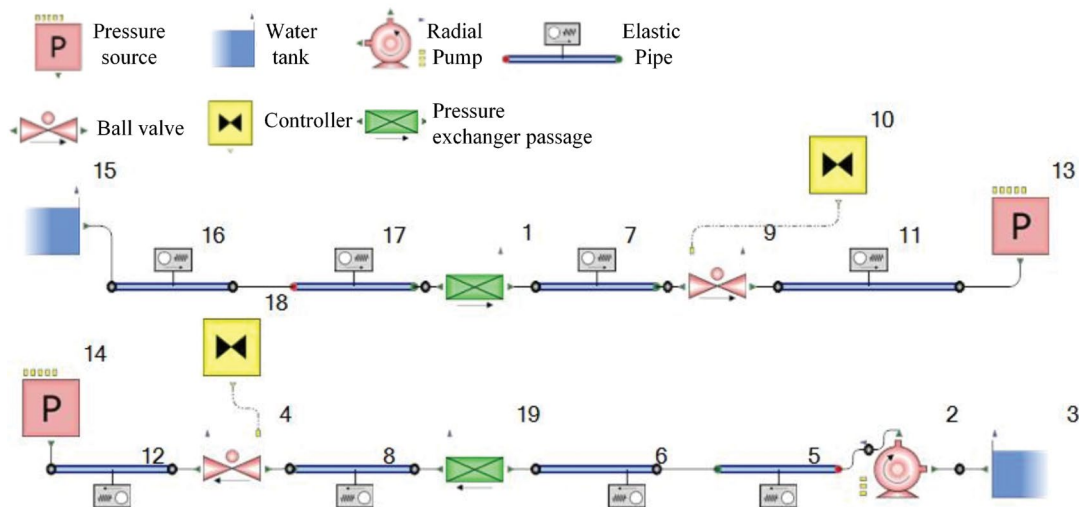


Fig. 10. Diagram of a pipeline system with valve action.

For the pipeline upstream, the fluid supply is adequate and can be regarded as a constant pressure source. With the closing of the downstream valves in high-pressure and low-pressure pipelines, the influence is shown in Fig. 11. As can be seen, a pressure surge is observed with the valve closing at 0.3 s, the compression wave propagates along the upstream, at the same time, the expansion wave propagates to the pipeline downstream. The wave amplitude of the high-pressure pipeline is much higher than that of the low-pressure pipeline. After the pressure surge caused by valve action, the wave fluctuation decreases gradually with the stability of the transient condition. At the same time, the fluctuation frequencies of the two pipelines are almost the same. This is because of the consistent settings of pipeline length, wave speed, and the synchronous valve action in both of the high pressure and the low-pressure pipelines.

For a practical desalination plant, the pressure fluctuation will affect the water production stability of the membrane process. Moreover, the repeated unexpected pressure surge may cause fatigue of the membrane material [16], and also may harm other components such as pipes, bends, pumps and pressure exchangers when exceeds their allowable pressure. Since the high-pressure and low-pressure areas in RPE are separated, the transient operation of one side will not affect the other side. Therefore, the overpressure in the downstream of one pipeline during the pressure exchange process will not cause hydraulic damage to the other pipeline. In view of this, the pressure fluctuation in the high-pressure pipeline is studied and the corresponding measures to reduce the pressure fluctuation are discussed.

As shown in Fig. 12, the slow closing valve operation changes the wave shape and reduces the fluctuation peak of the pressure wave. When the valve closing time changes from 0.01 s to 0.3 s, pressure peak value is decreased by about 50%, and the subsequent pressure fluctuations tend to become stable as before the valve operation. Hence, with valve slow closing action, the impact of water hammer wave on pipe

components can be well weakened, making the system and components safe and reliable during the transient operation.

Apart from the time length of valve closure, the closure scheme also impacts the pressure surge. When the total valve closure time is fixed, the valve opening can be adjusted through a combination of valve operation schemes. In a fast-slow closure scheme, the valve operates in a rapid closing followed by a slow closing action. Likewise, the valve shuts down slowly at first and then rapidly in a slow-fast closure scheme.

In Fig. 13 the time length for valve closure is 0.3 s for both schemes. In the fast-slow closure scheme, half of the valve closure is finished in the first 0.01s, and then fully closed in the following 0.29 s. The opposite operation sequence applies to the slow-fast closure scheme. It is seen that the pressure fluctuation of the slow-fast closure scheme has a similar pattern and almost equivalent peak pressure value compared

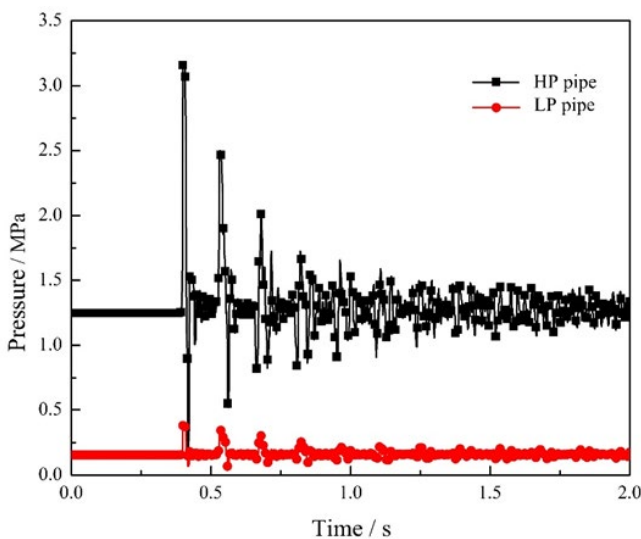


Fig. 11. Pressure fluctuations at high-pressure and low-pressure pipelines at fast valve closing.

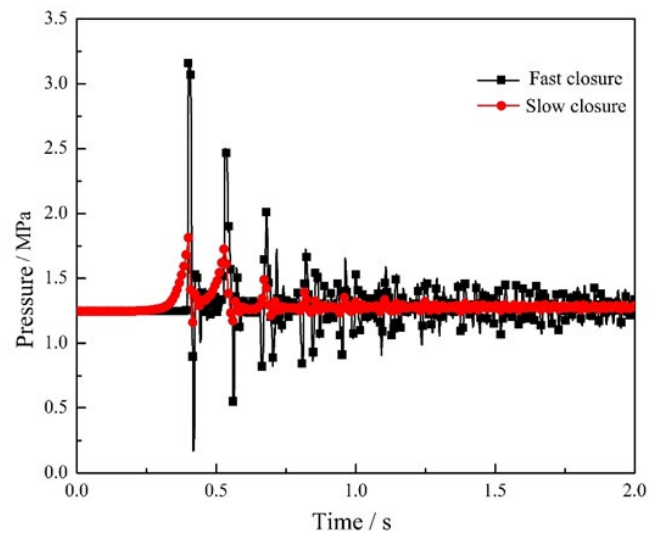


Fig. 12. Pressure fluctuations at high-pressure pipelines with different valve actions.

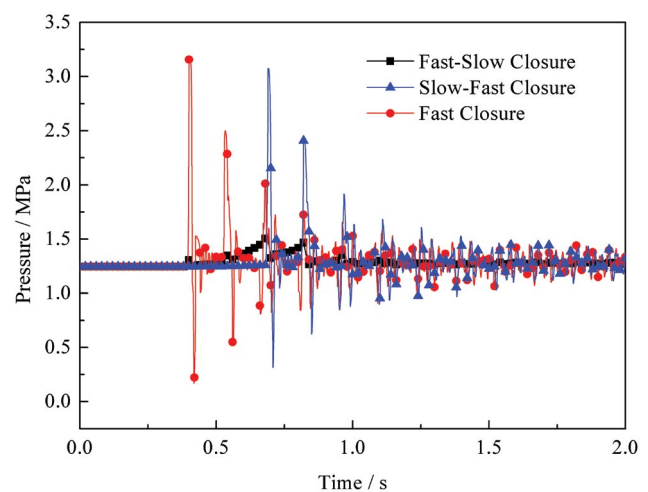


Fig. 13. Pressure fluctuations at low-pressure pipelines with different valve closure schemes.

to the fast closure scheme. While in the fast-slow closure scheme, the suppression of pressure fluctuation is observed, indicating the dominant effect of valve operation before the final closure of the valve.

Fig. 14 shows the effects of different valve operation schemes on the peak value of the pressure surge. For the fast-slow scheme with a total closure time of 0.3 s, the fast closure rate refers to the percentage of valve closure during the first rapid closure operation, which is set in a range of 30%~70%. The valve closure time for a fast closure scheme is set in a range of 0.1~0.8 s. It is seen that in the fast-slow closure scheme, the peak pressure maintains relatively lower until the valve closure time of the fast closure scheme extends to 0.5 s and longer. The simulation result shows that an optimum fast closure rate exists, and it is about 0.6 in our simulation case. Meanwhile, the peak pressure decreases significantly with valve closure time, which is in agreement with previous analysis. Therefore, it can be concluded that the closure time has a more obvious effect on pressure surge

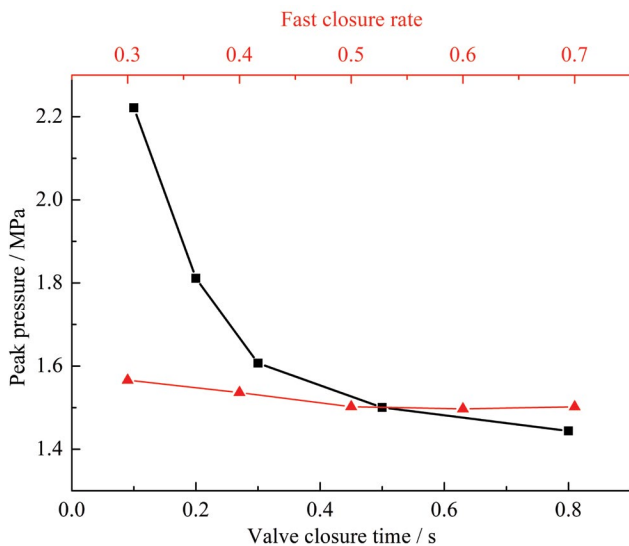


Fig. 14. Effects of valve closure schemes on peak pressure.

control. Moreover, for a fixed valve closure time, there exists an optimum fast closure rate that could reduce peak pressure to lower value.

3.4. Hydraulic performance of a subsystem

An example is studied representing a simple case based on a subsystem of a desalination plant, which contains several PX devices in an array operates at a common working condition. As is shown in Fig. 15, the subsystem also comprises high-pressure and low-pressure pipelines. In the PX array, six PX devices operate in parallel to recover the energy from high-pressure upstream. Valves 1~4 and valves 5~6 positioned downstream are used for different flow configurations and transient control, respectively. In accordance with a common SWRO process, the operating conditions are set as follows: the PX array connecting high-pressure pipeline maintains at a pressure above 6.5 MPa, the pressure for low-pressure pipeline is above 0.1 MPa. After model simulation under steady and transient conditions, the effects of pipe configuration and valve operation schemes on system hydraulic performance are analyzed.

Different valve status represents for different flow schemes of the subsystem. As an example of the high-pressure pipeline, closing valve V1 represents a Z flow scheme, whereas closing valve V3 represents a U flow scheme. In the Z flow scheme, the fluid stream flows into one end of the PX array and leaves from the other end, while the U flow means the fluid stream enters and leaves from the same end.

As is shown in Fig. 16, Case 1~Case 4 represents for Z flow for both pipelines; U flow for both pipelines; Z flow for high-pressure pipeline while U flow for low-pressure pipeline; and vice versa. It is seen that the pressure transfer efficiency reaches a maximum of 98.37% in a U flow scheme among all simulation cases, and the total pressure loss for both pipelines is lower at the same time. This is because in the U flow scheme, the pressure increases along the inflow direction of the inlet manifold when velocity decreases, and it decreases along the outflow direction of the outlet manifold when fluid starts to merge. This results

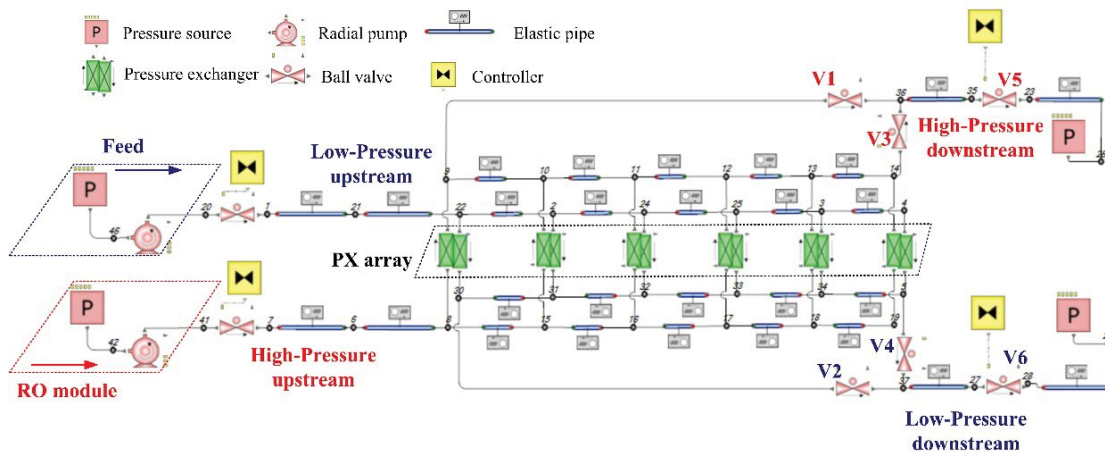


Fig. 15. Schematics of the subsystem model of a desalination process.

in a more even distribution of pressure drop and flow for each PX unit.

The effects of flow schemes and valve operations on pressure transient control are shown in Figs. 17 and 18. The valve closure time is set as 0.3 s, and the fast-slow closure is defined as a 60% shut down during the first 0.01 s, and the remaining 40% shunt down in the following 0.29 s. As an example from a low-pressure pipeline in Fig. 17, it is suggested that the pressure surge is more obvious for the Z flow scheme, and the fast-slow closure with U flow reduces pressure fluctuation significantly in comparison. In Fig. 18, it is seen that the peak pressures in the fast-slow closure scheme are 6.837 MPa for high-pressure pipelines and 0.4 MPa for the low-pressure pipeline, which represents the best operation scheme in comparison for pressure surge control.

4. Conclusions

This work presents a cross-scale co-simulation based on 1D MOC and 3D CFD coupling numerical simulation for the energy recovery process in the SWRO system. The accuracy of simulation in RPE device and calculation efficiency in pressure wave propagation in the pipeline system are both

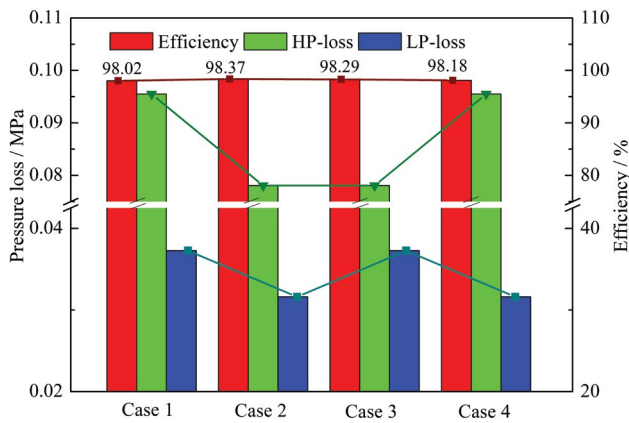


Fig. 16. Effects of flow schemes on system performance.

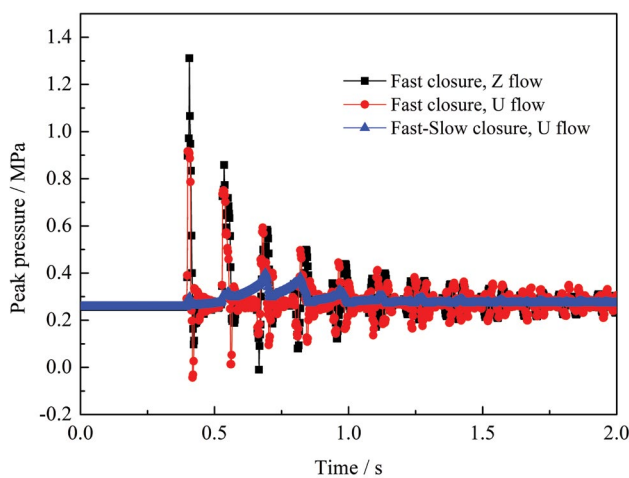


Fig. 17. Pressure variation in different operating schemes for low-pressure pipelines.

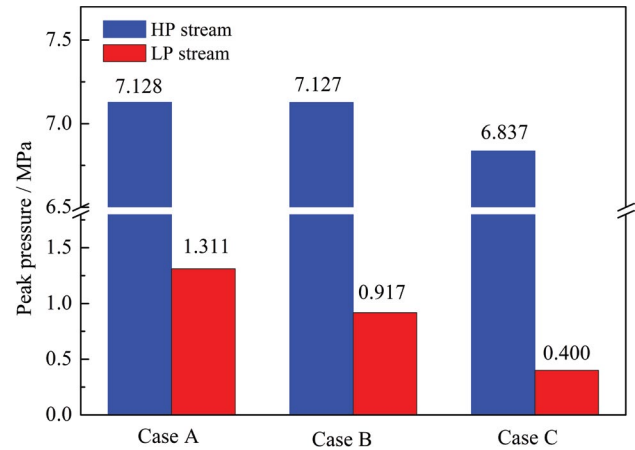


Fig. 18. Effects of operating schemes on peak pressure.

balanced with this method. The co-simulation performed by a self-programmed platform concludes that the reasonable correction factor and initial pressure value are important in the cross-scale coupling calculation, which will largely affect the convergence process. While the initial flow value and convergence factor will not have a significant impact on the calculation results. In addition, the pressure drops at the working condition of this study are about 0.13 MPa for the high-pressure area and 0.073 MPa for the low-pressure area of RPE respectively.

With the extracted modeling data, the suppression method of pressure fluctuation and valve arrangement effects were evaluated. The extension of valve closure time should be taken as the prior consideration for designers to suppress pressure fluctuation. For a fixed valve closure time due to the design limit, the fast-slow closure scheme can further reduce peak pressure. And there exists an optimum fast closure rate which is 60% in our study corresponds to the lowest peak pressure value. In addition, a U flow arrangement in the energy recovery subsystem is beneficial for better system performance in terms of a higher energy transfer efficiency and lower pressure surge value, which guarantees the efficiency and safety for system design.

Acknowledgment

This work was supported by the National Natural Science Foundation of China (Grant No. 21978227) and the Fundamental Research Funds for the Central Universities (Grant No. 1191329136).

References

- [1] M. Elimelech, W.A. Phillip, The future of seawater desalination: energy, technology, and the environment, *Science*, 333 (2011) 712–717.
- [2] R.L. Stover, Retrofits to improve desalination plants, *Desal. Wat. Treat.*, 13 (2010) 33–41.
- [3] R.L. Stover, Seawater reverse osmosis with isobaric energy recovery devices, *Desalination*, 203 (2007) 168–175.
- [4] E. Xu, Y. Wang, L. Wu, S. Xu, Y. Wang, S. Wang, Computational fluid dynamics simulation of brine-seawater mixing in a

- rotary energy recovery device, *Ind. Eng. Chem. Res.*, 53 (2014) 18304–18310.
- [5] K. Liu, J. Deng, F. Ye, Numerical simulation of flow structures in a rotary type energy recovery device, *Desalination*, 449 (2019) 101–110.
- [6] L. Jiao, Y. Shi, Z.C. Liu, L. Li, Z.M. Feng, C.F. Zhao, Y. Wei, Experimental research on pressure loss of rotary pressure exchanger, *IOP Conf. Ser.: Mater. Sci. Eng.*, 129 (2016) 012006.
- [7] O.M. Al-Hawaj, Theoretical analysis of sliding vane energy recovery device, *Desal. Wat. Treat.*, 36 (2011) 354–362.
- [8] F. Ye, J. Deng, K. Liu, Z. Cao, Performance study of a rotary vane pressure exchanger for SWRO, *Desal. Wat. Treat.*, 89 (2017) 36–46.
- [9] Z. Cao, J. Deng, Z. Chen, W. Yuan, Numerical analysis of the energy recovery process in a disc-type pressure exchanger with pressure-boost effect, *Desal. Wat. Treat.*, 105 (2018) 152–159.
- [10] N. Liu, Z. Liu, Y. Li, L. Sang, An optimization study on the seal structure of fully-rotary valve energy recovery device by CFD, *Desalination*, 459 (2019) 46–58.
- [11] Y. Wang, Y. Duan, J. Zhou, S. Xu, S. Wang, Introducing pre-pressurization/depressurization grooves to diminish flow fluctuations of a rotary energy recovery device: numerical simulation and validating experiment, *Desalination*, 413 (2017) 1–9.
- [12] P. Grafenberger, P. Klinner, P. Nefischer, F. Klingebiel, Simulation of engine cooling with coupled 1D and 3D flow computation, *Automobiltechnische Z.*, 102 (2000) 248–256.
- [13] A. Matin, Z. Khan, S.M.J. Zaidi, M.C. Boyce, Biofouling in reverse osmosis membranes for seawater desalination: phenomena and prevention, *Desalination*, 281 (2011) 1–16.
- [14] ERI Energy Recovery Inc., Installation, Operation & Maintenance Manual 65-Series Pressure Exchanger Energy Recovery Devices ERI® Document Number 80019–01 Revision 8, San Leandro, 2008.
- [15] R.L. Stover, A.O. Fernandez, J. Galtes, Permeate Recovery Rate Optimization at the Alicante Spain SWRO Plant, *Proc. International Desalination Association World Congress*, Dubai, UAE, 2009, DB09–083.
- [16] S.A. Avlonitis, D.A. Avlonitis, K. Kralis, A. Metaxa, Water hammer simulation in spiral wound reverse osmosis membranes, *Desal. Wat. Treat.*, 13 (2010) 74–81.